### A semiclassical model for orientation effects in electron transfer reactions

Robert J. Cave, Stephen J. Klippenstein, and R. A. Marcus

Arthur Amos Noyes Laboratory of Chemical Physics, California Institute of Technology, Pasadena,

California 91125

(Received 26 August 1985; accepted 12 December 1985)

An approximate solution to the single-particle Schrödinger equation with an oblate spheroidal potential well of finite depth is presented. The electronic matrix element  $H_{BA}$  for thermal electron transfer is calculated using these wave functions, and is compared with values of  $H_{BA}$  obtained using the exact solution of the same Schrödinger equation. The present method yields accurate results for  $H_{BA}$ , within the oblate spheroidal potential well model, and is useful for examining the orientational effects of the two centers on the rate of electron transfer.

### I. INTRODUCTION

Increased understanding of biological redox systems has led to the need for detailed information regarding the effects of mutual orientation and separation distance on the rate of electron transfer. The nonspherical structure of many biological redox components, such as hemes, chlorophyll a and b, and quinones leads one to expect that the mutual orientation of redox partners can significantly affect the rate of electron transfer.

Examples of systems for which orientational effects are expected include electron transfers involving cytochrome c as well as various components in photosynthetic reaction centers. It will be recalled that cytochrome c is a complex in which a heme lies in a crevice created by a surrounding protein and is bonded to the protein by thioether bridges. It is believed that electron transfers to and from the heme occur predominantly near the opening of the crevice to the solution.

Several previous studies have attempted to qualitatively assess orientational effects using simplified models.<sup>2</sup> Recently, Siders et al.<sup>3</sup> developed a model for examining orientation effects in transfers between large, aromatic molecules, where the high lying electrons are delocalized, and have applied<sup>4</sup> it to several systems of current experimental interest. The basis of the model is the calculation of single-site, one-electron wave functions of oblate-spheroidal wells having constant potentials. These wave functions are then used to calculate the electron-transfer matrix element, the predominant distance dependent quantity in theories of nonadiabatic electron transfer.

In the present paper two simple approximations to this model are introduced. The resulting approximate model is computationally much faster, conceptually simpler, and will be seen to yield accurate results for  $H_{BA}$ , within the original model. The paper is organized as follows. The exact model and the form of the electron-transfer matrix element are outlined in Sec. II. The exact wave functions for the original model<sup>3</sup> are described in Sec. III and the two additional approximations are introduced in Sec. IV. The calculation of  $H_{BA}$  and the energy quantization for the approximate wave

functions are briefly discussed there. The exact and approximate results for the wave function and the electron-transfer matrix element are compared and discussed in Sec. V, with concluding remarks made in Sec. VI.

#### II. THE THEORETICAL MODEL

The present model<sup>3</sup> is intended to describe electron transfer between two fixed sites, A and B. In the zeroth-order problem A and B do not interact and only the transferable electron is considered explicitly, i.e., each electronic wave function is a one-electron wave function. The states localized at sites A and B are labeled  $\Psi^A$  and  $\Psi^B$ , respectively. The model has been designed to assess orientational effects, at various distances, in electron transfer between large aromatic systems and it is thus assumed that the transferable electron is delocalized over the aromatic ring system.

Each isolated site is modeled as an oblate spheroid of constant negative potential inside the well and zero potential outside the well. Thus, in oblate spheroidal coordinates<sup>5</sup>  $(\xi,\eta,\varphi)$  the potential V is a constant,  $-V_0$ , inside the well  $(\xi \leqslant \xi_0)$ , and another constant (V=0) outside,<sup>3</sup> and is depicted in Fig. 1. The molecule is taken to lie in the xy plane of the spheroid; a (in Fig. 1) is chosen as an approximate inplane radius of the molecule, and b is chosen to yield a reasonable thickness for the electronic orbital of interest. The usual Cartesian coordinates are readily defined in terms of these coordinates [Eq. (2) of Ref. 3].

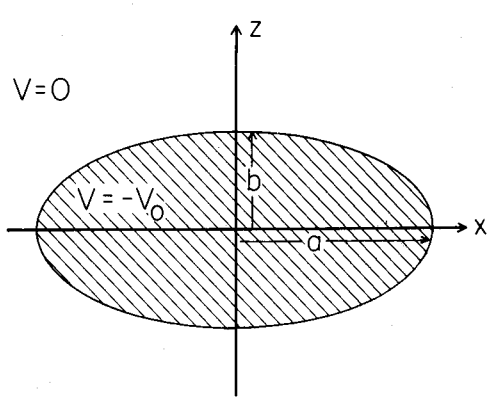


FIG. 1. Potential well for a single site. There is cylindrical symmetry about the z axis. On the well boundary the coordinate  $\xi$  equals  $\xi_0$ .

a) Contribution No. 7267

The single-site one-electron Schrödinger equation may be written as

$$(\nabla^2 + k^2)\Psi = 0, \tag{1}$$

where  $k^2$  equals  $2\mu(E+V_0)/\hbar^2 \equiv k_i^2$  inside the well and  $2\mu E/\hbar^2 \equiv k_0^2$  outside. A choice of  $V_0$  yields a specific value of an orbital's energy E upon quantization.

The rate of nonadiabatic electron transfer between two such localized fixed states  $A \rightarrow B$  may be written as  $^{6-8}$ 

$$k_{A\to B} = \frac{2\pi}{\hbar} |T_{BA}|^2 (FC), \qquad (2)$$

where (FC) is a Franck-Condon sum, discussed in detail elsewhere, e.g., Refs. 8-10.  $T_{BA}$  is the electronic matrix element which, in the present model, was expressed in terms of  $H_{BA}$ ,  $H_{AA}$ , and  $S_{AB}$  as

$$T_{BA} = (H_{BA} - S_{AB}H_{AA})/(1 - |S_{AB}|^2),$$
 (3a)

$$H_{BA} = \int \Psi^{B*} V^{B} \Psi^{A} d\tau, \quad H_{AA} = \int \Psi^{A*} V^{B} \Psi^{A} d\tau,$$
 (3b)

$$S_{AB} = \int \Psi^{A*} \Psi^{B} d\tau, \qquad (3c)$$

where  $V^B$  is the potential of the transferable electron for the isolated site B.  $T_{BA}$  is the primary distance and orientation dependent quantity in the expression for  $k_{A\rightarrow B}$ .  $T_{BA}$  was found<sup>3</sup> to agree with  $H_{BA}$  when  $H_{BA}$  was nonzero to within 3% for states similar to those examined here, when the wells were in contact and the agreement improved with increasing separation distance. Furthermore, the zeros of  $T_{BA}$  and  $H_{BA}$  were within 2° of one another (for a specific state examined).<sup>4</sup> Since the evaluation of  $T_{BA}$  requires considerably more computational time, only  $H_{BA}$  is calculated here.

The present model was developed to obtain approximate expressions for  $\Psi^A$  and  $\Psi^B$  and thereby to significantly simplify the calculation of  $H_{BA}$ . To facilitate the description of the two approximations introduced below, the calculation of the exact wave function is outlined briefly first.

### **III. THE EXACT SINGLE-WELL EIGENFUNCTIONS**

In the oblate spheroidal coordinate system, Eq. (1) is separable.<sup>5</sup> Therefore, assuming that  $\Psi \equiv \Psi_{mn}(\xi, \eta, \varphi) = R_{mn}(\xi)S_{mn}(\eta)\Phi_m(\varphi)$  one obtains the separated equations<sup>5</sup>

$$\frac{d^2\Phi_m}{dm^2} + m^2\Phi_m = 0, (4a)$$

$$\frac{d}{d\eta}\left\{ (1-\eta^2) \frac{dS_{mn}^i}{d\eta} \right\} + \left\{ \frac{d^2}{4} \eta^2 k_i^2 - \frac{m^2}{1-\eta^2} \right\}$$

$$+\lambda_{mn}^{i}\left\{ S_{mn}^{i}=0,\right. \tag{4b}$$

$$\frac{d}{d\xi} \left\{ (1 + \xi^2) \frac{dR_{mn}^i}{d\xi} \right\} + \left\{ \frac{d^2}{4} \xi^2 k_i^2 + \frac{m^2}{1 + \xi^2} - \lambda_{mn}^i \right\} R_{mn}^i = 0,$$
(4c)

where  $d = 2\sqrt{a^2 - b^2}$ , and  $m^2$  and  $\lambda_{mn}^i$  are separation constants. The superscript *i* indicates a function appropriate to the potential region inside the well  $(\xi \leqslant \xi_0)$ , while a super-

script o will indicate these properties outside  $(\xi > \xi_0)$ .  $\Phi_m(\varphi)$  is equal to  $A \sin m\varphi + B \cos m\varphi$ , and since  $\Phi_m$  must be single valued, m is an integer. The index n orders the eigenvalues  $\lambda_{mn}$  in order of increasing value and is chosen to have the possible values  $n = m, m + 1, m + 2, \dots$ . This choice is convenient since in the spherical limit, where a tends to b, the eigenfunction given below reduces to a single term  $\Psi_{mn}$  with n = l, l being the angular momentum quantum number of the particle for the spherical case.

Since the method is primarily designed to assess orientation effects in electron transfers between delocalized  $\pi$  systems, only states with no  $\xi$ -type nodes, and one  $\eta$ -type node are considered.<sup>4</sup> These states are odd with respect to reflection in the xy plane and are labeled  $(m,\pi)$ ; they are  $\pi$ -like states with azimuthal quantum number m. (A more complete description of the states is given elsewhere.<sup>3,4</sup>)

To satisfy the quantization conditions, namely the continuity of the wave function and of its normal derivative at the well boundary, the exact solution  $\Psi_{m,\pi}$  is written as a linear combination of the separated solutions,<sup>3</sup> that is, as  $\sum_{r=0}^{\infty} C_n^i \Psi_{mn}^i$  for  $\xi \leqslant \xi_0$ , and as  $\sum_{r=0}^{\infty} C_n^0 \Psi_{mn}^0$  for  $\xi \geqslant \xi_0$ . Here, n=2r+m+1. Quantization is accomplished by iterating the energy E until  $\Psi_{m,\pi}$  and its derivative are continuous at the well boundary  $\xi = \xi_0$ .

# IV. APPROXIMATE SINGLE-WELL EIGENFUNCTIONS AND $H_{BA}$ CALCULATION

The two new approximations made in the present paper to obtain single-well functions for use in calculating  $H_{BA}$  are the following: (1) The sums for the inner and outer quantized wave functions are each truncated to a single term, one inside and one outside the well, and (2) each  $R_{mn}$  and  $S_{mn}$ , inside and outside the well, is evaluated semiclassically rather than as a sum of known special functions.

The first approximation was prompted by two observations: (a) In the spherical limit the inner and outer wave functions are each represented by a single mn term. (For the case of  $\pi$ -like states this single term has n=m+1.3) Since an oblate spheroid can be viewed as a "flattened sphere" it is reasonable that the use of only one term in the sum will be adequate when the eccentricity is not too high. (b) Empirically, we noted in our numerical calculations<sup>3,4</sup> that both inside and outside the potential well it was common for a single  $C_n^i$  and a single  $C_n^o$  to dominate the other coefficients for the states considered.

In view of approximation (1) above, the total wave function, for the  $(m,\pi)$  states of interest here may now be written as

$$\Psi_{m,\pi} \cong \begin{cases} C_{m+1}^{i} \Psi_{m,m+1}^{i}(\xi,\eta,\varphi); & \xi < \xi_{0} \\ C_{m+1}^{o} \Psi_{m,m+1}^{o}(\xi,\eta,\varphi); & \xi > \xi_{0}. \end{cases}$$
 (5)

Within this approximation the quantization conditions can now be satisfied only approximately at the well boundary:

$$C_{m+1}^{i}\Psi_{m,m+1}^{i} \cong C_{m+1}^{o}\Psi_{m,m+1}^{o} \quad (\xi = \xi_{0}),$$
 (6a)

$$C_{m+1}^{i} \frac{\partial \Psi_{m,m+1}^{i}}{\partial \xi} \bigg|_{\xi=\xi_{0}} \cong C_{m+1}^{o} \frac{\partial \Psi_{m,m+1}^{o}}{\partial \xi} \bigg|_{\xi=\xi_{0}}.$$
 (6b)

To satisfy Eq. (6a) both sides were squared and then integrated over  $\eta$  and  $\varphi$  at  $\xi = \xi_0$ , thereby averaging over the

boundary. Taking the square root, and following the same procedure for Eq. (6b) one obtains an equality of  $C^i_{m+1}R^i_{m,m+1}(\xi_0)$  and of  $C^o_{m+1}R^o_{m,m+1}(\xi_0)$  and also of their derivatives, when  $S^i_{m,m+1}, S^o_{m,m+1}$  and  $\Phi_m$  are each normalized to unity. Thereby, the ratio yields

$$\frac{1}{R_{m,m+1}^{i}(\xi)} \frac{d}{d\xi} R_{m,m+1}^{i}(\xi)|_{\xi=\xi_{0}}$$

$$= \frac{1}{R_{m,m+1}^{o}(\xi)} \frac{d}{d\xi} R_{m,m+1}^{o}(\xi)|_{\xi=\xi_{0}}.$$
(7)

This equation serves to determine the approximate singlesite wave function to within a normalization constant (Appendix A).

A semiclassical approximation is now introduced to simplify evaluation of  $R_{mn}$  and  $S_{mn}$  both inside and outside the well. In previous applications 3,4 the individual inner and outer  $R_{mn}$ 's and inner and outer  $S_{mn}$ 's were evaluated instead through series expansions in spherical Bessel functions and associated Legendre functions,5,11 a process which can be time consuming. In the present study, semiclassical approximations were used for  $S_{mn}^{i}$ ,  $S_{mn}^{o}$ ,  $R_{mn}^{i}$ , and  $R_{mn}^{o}$  (uniform semiclassical approximations for the first two and primitive for the latter two, for reasons given in Appendix A). The resulting functions are seen (in Tables II, III, V, and VI given later) to be accurate. Previous uniform semiclassical approximations to prolate spheroidal wave functions, described by Sink and Eu, 12 have a number of differences from ours. 13 Our expressions for the wave functions and the procedure for calculating  $H_{BA}$  are given in Appendix A. The semiclassical treatment of  $S_{mn}^{i}(\eta)$  itself involves four turning points for the states of interest in the present article.

The general procedure used for calculations of  $H_{BA}$  (both approximate and exact) was to choose a value for E which yielded the desired decay of  $H_{BA}$  with distance, after adjusting  $V_0$ . Thus, an accurate quantization of the energy for a given value of the potential was not needed. What is required is, given this decay, that the orientation dependence of  $H_{BA}$  be accurate for the states of interest. Nevertheless, for completeness, results for quantization of E are given in Appendix B.

### V. RESULTS AND DISCUSSION

In this section the exact and approximate results for  $H_{BA}$  are compared and discussed for a number of states of interest. The physical significance of these  $(m,\pi)$  states was discussed earlier.<sup>3,4</sup> In particular,  $(4,\pi)$  states are used to model the HOMO's of porphyrin derivatives and  $(5,\pi)$  states to model the LUMO's in such molecules. The value of E (and hence of  $V_0$ ) is chosen so as to give a fall off with distance of the rate which is fairly consistent with presently available data. The exact<sup>3,4</sup> and approximate electronic matrix elements  $H_{BA}$  so calculated are compared below in Table I and in Figs. 3, 4, and 6.

To describe the orientation of the two wells for the calculation of  $H_{BA}$  the  $(R,\Theta)$  coordinate system shown in Fig. 2 is used. Unless otherwise specified, the xy planes of both wells are chosen to be parallel and the centers of the wells are

TABLE I. Exact and approximate  $H_{BA}$ 's for a pair of  $(4,\pi)$  states as a function of distance at  $\Theta = 0^{\circ}$  and  $\Theta = 90^{\circ}$ .

Θ (deg)	R(Å)	H <sub>BA</sub> a	$H^{\mathrm{sc}}_{BA}{}^{\mathrm{b}}$	$H_{BA}^{ m sphere\ c}$
0°	10	3.8( - 4) d	3.0( - 4)	7.0( - 4)
•	15	2.0(-6)	1.8(-6)	2.2(-6)
	20	2.2(-8)	2.1(-8)	2.0(-8)
	25	3.8(-10)	3.7(-10)	3.0( - 10
90°	10	-4.1(-2)	-5.8(-2)	-9.9(-3)
	15	-1.3(-4)	-1.5(-4)	<b> 4.5( 5)</b>
	20	-1.5(-6)	-1.7(-6)	-5.8(-7)
	25	-3.0(-8)	-3.4(-8)	-1.2(-8)

<sup>&</sup>lt;sup>a</sup> For each  $(4,\pi)$  state E = -1.1525 eV,  $V_0 = 17.352$  97 eV, a = 4.85 Å,

held at a given separation distance R. The angle  $\Theta = 0^{\circ}$  (Fig. 2) corresponds to a "face-to-face" configuration and  $\Theta = 90^{\circ}$  to an "edge-to-edge" one.

The exact and approximate  $H_{BA}$ 's are presented as functions of distance for transfer between two  $(4,\pi)$  states, for the  $\Theta=0^\circ$  and  $\Theta=90^\circ$  orientations in Table I. The agreement is seen to be good. The deviation in Table I is largest at small R, and, especially in the  $\Theta=0^\circ$  orientation, is due to the contribution of other states in the exact state sum over  $R_{mn}S_{mn}$  [cf. Eq. (6) of Ref. 3] at these small R's. It is clear that this contribution from other n's is only serious at very small R. For comparison, results using spherical wells of similar volume and energy are also given in Table I. They are seen to be significantly less accurate than the present approximation to the spheroidal problem, particularly at  $\Theta=0^\circ$ .

In Fig. 3 exact and approximate results for transfer between two  $(5,\pi)$  states are compared at constant edge-to-edge distance for various  $\Theta$ 's. As the edge-to-edge distance increases from 0 to 4 Å, the accuracy of the present approxi-

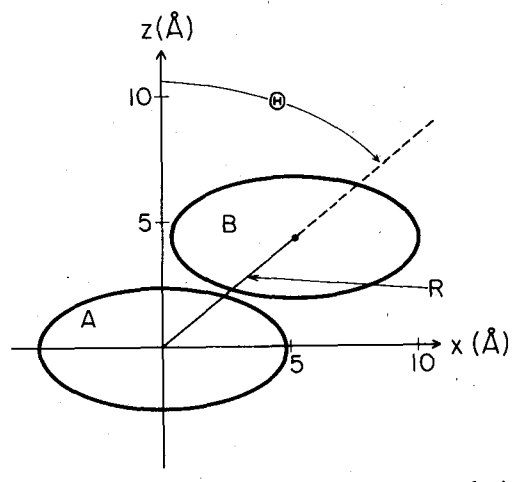


FIG. 2. Coordinate system used to specify the mutual orientation of wells A and B. The x axes of the wells are parallel and lie in the plane of the figure, as do the z axes.

 $<sup>^{</sup>b}$  For each  $(4,\pi)$  state E=-1.1525 eV,  $V_{0}=17.541$  21 eV, a=4.85 Å, b=2.55 Å.

<sup>°</sup>For each  $(4,\pi)$  spherical state E=-1.1525 eV,  $V_0=18.0313$  eV, r=3.915 Å.

<sup>&</sup>lt;sup>d</sup>The numbers in parentheses are the powers of ten by which each entry should be multiplied.

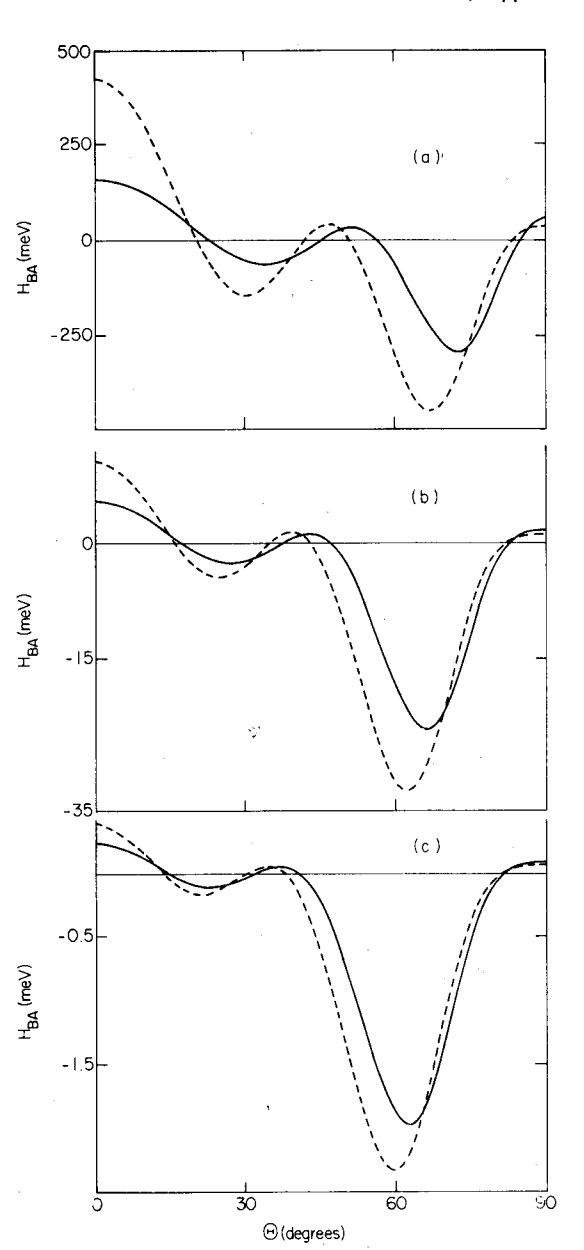


FIG. 3. The matrix element  $H_{BA}$  as a function of  $\Theta$  at several fixed edge-to-edge separations for  $(5,\pi) \rightarrow (5,\pi)$  transfer. For the donor and acceptor states a=5 Å, b=2 Å, E=-2.8 eV. --- corresponds to the exact calculations where  $V_0=26.3022$  eV. — corresponds to the semiclassical calculations where  $V_0=25.532$  eV. (a) Edge-to-edge separation is 0 Å. (b) Edge-to-edge separation is 2 Å. (c) Edge-to-edge separation is 4 Å.

mate calculation also increases. The agreement is good for an edge-to-edge distance of 4 Å, and for larger separations the agreement remains good.

In Fig. 4  $H_{BA}$ 's for the same set of orientations are given for transfer between  $(5,\pi)$  and  $(4,\pi)$  states. Calculations similar to those in Figs. 3 and 4 have been used previously<sup>3,4</sup> to model the orientation dependence of the electron transfer rate between two porphyrins. Again, at all distances the approximate results for the  $H_{BA}$ 's show similar behavior to the exact ones and for an edge-to-edge separation of 4 Å or larger the agreement is good.

Results for a different class of orientations (cf. Fig. 5) are given in Fig. 6. For these results, the wells are held at a given R, in the edge-to-edge ( $\Theta = 90^{\circ}$ ) orientation, but the

xy planes are twisted about the line of centers through an angle  $\gamma$  relative to each other. The agreement is again good at all distances.

The present approximation has several advantages over the exact method developed in Ref. 3: (1) The present method is easier to implement. In the exact method the individual inner and outer  $R_{mn}$ 's and inner and outer  $S_{mn}$ 's were constructed as sums of known special functions. Each sum was then checked for convergence at all values of the argument for which the function was evaluated. Moreover, the total wave function was itself (in principle) an infinite sum which had to be checked for convergence at each evaluation. In the present method each inner and outer  $R_{mn}$  and each inner and

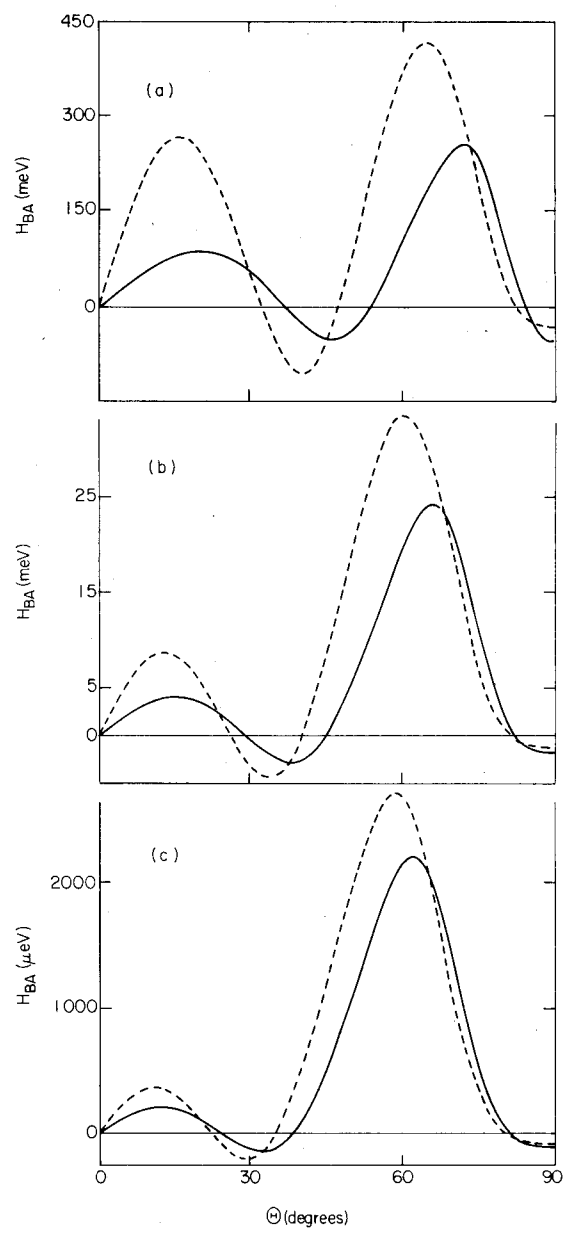


FIG. 4. The matrix element  $H_{BA}$  as a function of  $\Theta$  at several fixed edge-to-edge separations for  $(5,\pi) \rightarrow (4,\pi)$  transfer. For the donor and acceptor states a=5 Å, b=2 Å, E=-2.8 eV. For the exact calculations (--) the donor  $V_0$  is 26.3022 eV and the acceptor  $V_0$  is 22.199 eV. For the semiclassical calculations (—) the donor  $V_0$  is 25.532 eV and the acceptor  $V_0$  is 21.499 eV. (a) Edge-to-edge separation is 0 Å. (b) Edge-to-edge separation is 2 Å. (c) Edge-to-edge separation is 4 Å.

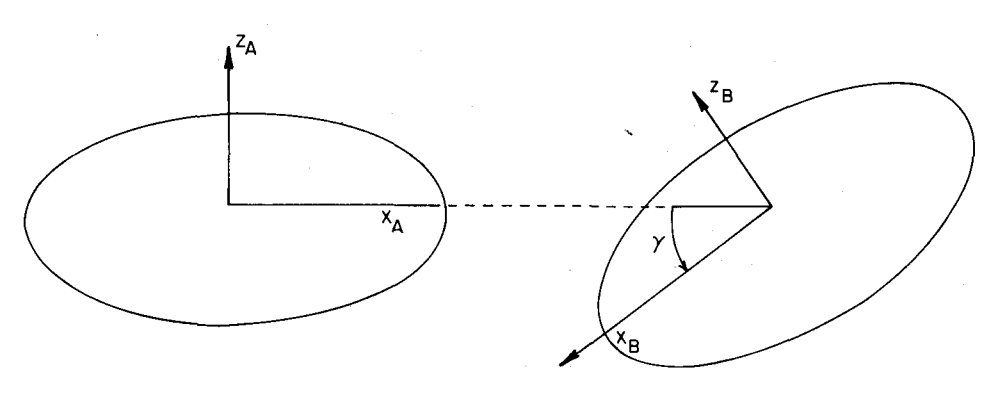


FIG. 5. Coordinate system used to specify the mutual orientation of the wells for the calculations presented in Fig. 6. The x axes of the wells lie in the plane of the figure. For  $\gamma = 0^{\circ}$  the x axes lie along the same line but are antiparallel.

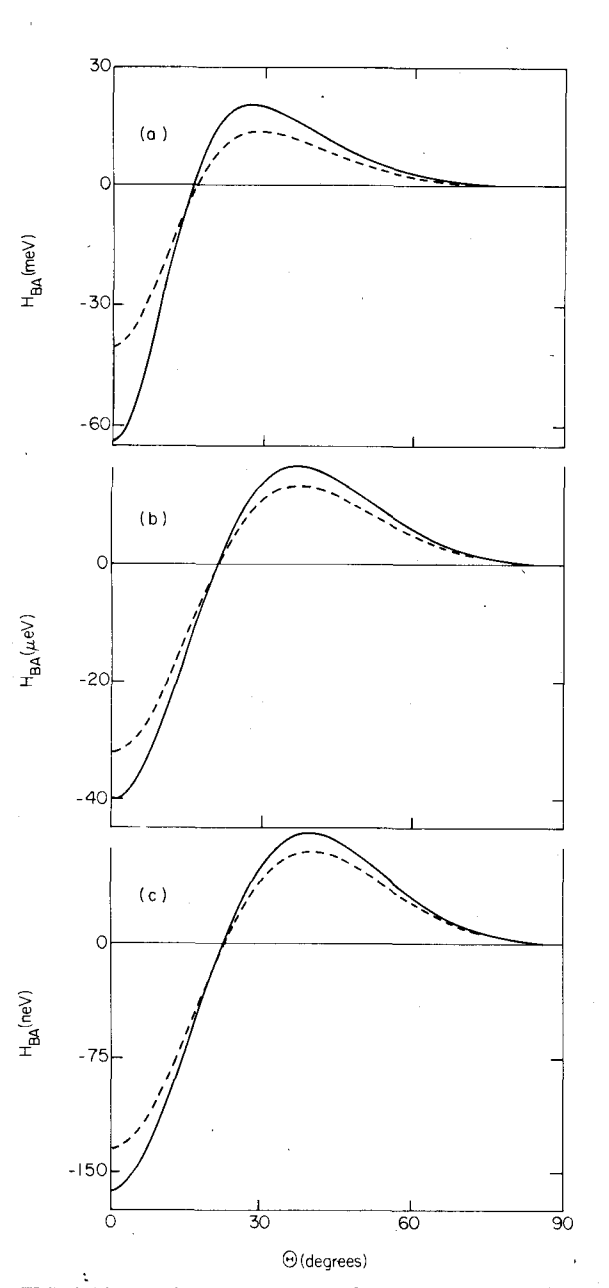


FIG. 6. The matrix element  $H_{BA}$  as a function of  $\gamma$  at several fixed edge-to-edge separations for  $(5,\pi) \rightarrow (5,\pi)$  transfer. For the donor and acceptor states a=5 Å, b=2 Å, E=-1.867 eV. For the exact calculations (---) the donor and acceptor  $V_0$  is 25.191 eV. For the semiclassical calculations (—) the donor and acceptor  $V_0$  is 24.438 eV. (a) Edge-to-edge separation is 0 Å. (b) Edge-to-edge separation is 5 Å. (c) Edge-to-edge separation is 10 Å.

outer  $S_{mn}$  is evaluated as a single term, with convergence needed only for the respective integrals involved in the semiclassical expressions. The problem of convergence of a sum thus disappears. (2) The current method is considerably faster computationally. For each geometry in Figs. 3, 4, and 6, and Table I, the current method, treating  $H_{BA}$  as a threedimensional volume integral, required about 10 min CPU time (VAX 11-780) while the exact method required about 50 times longer. 14 (A method of reducing computation time for the exact method by reducing the dimensionality of the  $H_{BA}$  integral is given in Ref. 4. It could be adapted using the present approximations to the wave functions, but we have not done so. It is expected to give essentially the same results as the present three-dimensional integration.) (3) The accuracy of the present method supports the simple conceptual previously introduced<sup>3,4</sup> to understand the orientation dependence of  $H_{BA}$ . Previously, this simple conceptual model was understood<sup>3</sup> by analogy with results from the use of spherical wells, where the inner and outer wave functions are each single terms. The spheroidal functions were envisioned as distorted spherical functions. Here, a related assumption is made explicitly by treating the inner and outer  $\Psi$ 's as sin-

TABLE II. Relative values of  $S_{mn}^{0}(\eta)$ 's for various  $\eta$ 's.

η	m = 5, n =	= 6ª	$m=4, n=5^{\rm b}$		
	Semiclassical <sup>c</sup>	Exact	Semiclassical <sup>c</sup>	Exact	
0.9	9.83(1) <sup>d</sup>	9.83(1)	1.93(1)	1.92(1)	
0.8	4.71(2)	4.70(2)	6.81(1)	6.79(1)	
0.7	1.06(3)	1.06(3)	1.30(2)	1.30(2)	
0.6	1.71(3)	1.71(3)	1.89(2)	1.89(2)	
0.5	2.24(3)	2.24(3)	2.31(2)	2.31(2)	
0.4	2.48(3)	2.48(3)	2.44(2)	2.44(2)	
0.3	2.36(3)	2.36(3)	2.23(2)	2.23(2)	
0.2	1.84(3)	1.84(3)	1.70(2)	1.70(2)	
0.1	1.01(3)	1.01(3)	9.21(1)	9.21(1)	

<sup>&</sup>lt;sup>a</sup> For both exact and semiclassical cases, E = -2.8 eV,  $V_0 = 26.3022$  eV, a = 5 Å, b = 2 Å,  $\lambda_{56}^{0,ex} = 44.95$ ,  $\lambda_{56}^{0,ex} = 45.17$ .

<sup>&</sup>lt;sup>b</sup> For both exact and semiclassical cases, E = -2.8 eV,  $V_0 = 22.1985$  eV, a = 5 Å, b = 2 Å,  $\lambda_{45}^{0,ex} = 33.36$ ,  $\lambda_{45}^{0,sc} = 33.67$ .

<sup>&</sup>lt;sup>c</sup> The semiclassical function was set equal to the exact function at  $\eta=0.4$ . This was done for comparison purposes only and is not required for the  $H_{BA}$  calculations presented here.

<sup>&</sup>lt;sup>d</sup> The numbers in parentheses are the powers of ten by which each entry should be multiplied.

TABLE III. Relative values of  $S_{mn}^{i}(\eta)$ 's for various  $\eta$ 's.

-	m = 5, n =	= 6ª	$m=4, n=5^{\rm b}$		
η	Semiclassical <sup>c</sup>	Exact	Semiclassical <sup>c</sup>	Exact	
0.9	8.03(3) <sup>d</sup>	8.03(3)	1.28(3)	1.28(3)	
0.8	1.78(4)	1.78(4)	2.15(3)	2.16(3)	
0.7	1.94(4)	1.94(4)	2.07(3)	2.07(3)	
0.6	1.60(4)	1.60(4)	1.58(3)	1.59(3)	
0.5	1.13(4)	1.14(4)	1.08(3)	1.08(3)	
0.4	7.35(3)	7.36(3)	6.81(2)	6.84(2)	
0.3	4.44(3)	4.45(3)	4.06(2)	4.08(2)	
0.2	2.45(3)	2.46(3)	2.23(2)	2.25(2)	
0.1	1.08(3)	1.09(3)	9.79(1)	9.88(1)	

<sup>&</sup>lt;sup>a</sup> E,  $V_0$ , a, and b are the same as for the m = 5, n = 6 state of Table II.  $\lambda_{56}^{i,ex} = -0.1111$ ,  $\lambda_{56}^{i,ex} = 0.4718$ .

gle-term functions. The accuracy of these results therefore supports this model.

Although the goal of this paper is the calculation of  $H_{BA}$ 's, it is interesting to also compare the shape of the wave functions used with the exact ones. We do this next. More precisely we select the principal  $R_{mn}S_{mn}$  term in the exact sum (largest coefficient) and compare (in Tables II to VI given later) its  $R_{mn}$  and  $S_{mn}$ , inside and outside the well, with those of the corresponding approximate functions used in the present single-term calculation of  $H_{BA}$ . They are compared on a relative basis to emphasize their similar shape. (Normalized wave functions were, as already noted, used to calculate  $H_{BA}$ .) Also included in these comparisons are the exact and semiclassical  $\lambda_{mn}$ 's inside and outside the well.

The exact and approximate results for the  $S_{mn}^o$ 's and  $\lambda_{mn}^o$ 's for two of the states used in the present  $H_{BA}$  calculations are compared in Table II. The agreement for the  $S_{mn}^o$ 's and for the  $\lambda_{mn}^o$ 's is generally better than 1%. In Table III, exact and approximate  $S_{mn}^i$ 's and  $\lambda_{mn}^i$ 's are compared for the same two states. The agreement for the  $S_{mn}^i$ 's is again excellent, the largest error being less than 1%. (The agreement for both the  $R_{mn}^o$ 's and  $R_{mn}^i$ 's, discussed later, is also good.) The  $\lambda_{mn}^i$ 's themselves are somewhat inaccurate, though the splittings are in good agreement with those of the exact  $\lambda_{mn}^i$ 's (Table IV). (A similar problem was encoun-

TABLE V. Relative values of  $R_{mn}^{0}(\xi)$ 's for various  $\xi$ 's.

	m = 5,n	= 6 <sup>a</sup>	$m=4, n=5^{\rm b}$		
Ė	Semiclassical <sup>c</sup>	Exact	Semiclassical <sup>c</sup>	Exact	
1.0	3.47(-2) d	3.47( - 2)	1.44( - 2)	1.44( - 2)	
2.0	2.03(-4)	2.05(-4)	1.12(-4)	1.13(-4)	
3.0	1.86(-6)	1.88(-6)	1.20(-6)	1.21(-6)	
4.0	2.19(-8)	2.21(-8)	1.55(-8)	1.57(-8)	
5.0	2.97(-10)	3.00(-10)	2.23(-10)	2.27(-10)	
6.0	4.38(-12)	4.43(-12)	3.44(-12)	3.50(-12)	
7.0	6.83(-14)	6.90(-14)	5.53(-14)	5.63(-14)	
8.0	1.11( - 15)	1.12(-15)	9.18(-16)	9.35( - 16)	

<sup>&</sup>lt;sup>a</sup>E,  $V_0$ , a, and b are the same as for the m = 5, n = 6 state of Table II.  $\lambda_{56}^{0,\text{ex}} = 44.95$ ,  $\lambda_{56}^{0,\text{ex}} = 45.17$ .

tered by Sink and Eu in the prolate spheroidal problem. 12) The inaccuracy is seen, however, not to seriously affect the semiclassical  $S^{i}_{mn}$ 's and  $R^{i}_{mn}$ 's.

The exact and semiclassical  $R_{mn}^o$ 's are compared in Table V for the same two states as in Tables II and III. For comparison purposes, the functions are equated at the smallest  $\xi$ . The agreement is good over the entire region of interest. Similar accuracy is obtained for other states. The  $\lambda_{mn}^o$  values used in the calculations of  $R_{mn}^o$ 's for Table V were from exact and semiclassical methods, respectively. The exact and semiclassical  $R_{mn}^i$ 's are compared in Table VI. The agreement is again good and similar accuracy can be expected for other states.

The accuracy of the semiclassical functions and the agreement of the semiclassical and exact  $H_{BA}$ 's indicate that the relevant shapes of the semiclassical and exact wave functions are quite similar. The shapes of the exact  $(4,\pi)$  and  $(5,\pi)$  states are compared elsewhere<sup>4</sup> to the shapes of porphyrin HOMO's and LUMO's obtained in molecular orbital calculations and are found to be in qualitative agreement. It would be useful to compare also the present  $H_{BA}$  results with calculations which might be based on the corresponding molecular orbital wave functions. For face-to-face orientations  $T_{BA}$  has been evaluated using molecular orbital techniques. <sup>15,16</sup> Molecular orbital calculations of  $H_{BA}$  have not

TABLE IV. Corrected  $\lambda_{mn}^{i}$ 's.

	$m=5^{a}$			$m=4^{\rm b}$	
$\lambda_{ij}^{i}$	Exact	Semiclassical	$\lambda_{ij}^{i}$	Exact	Semiclassical
λ ;	- 0.293	0.381	λ i 44	- 9.49	- 8.85
λ 36	-0.111	0.562	$\lambda_{45}^{i}$	<b>- 9.37</b>	-8.73
$\lambda_{56}^{i} - \lambda_{55}^{i}$	0.182	0.181	$\lambda_{45}^{i} - \lambda_{44}^{i}$	0.12	0.12

<sup>&</sup>lt;sup>a</sup>E,  $V_0$ , a, and b are the same as for the m = 5, n = 6 state of Table II.

<sup>&</sup>lt;sup>b</sup> E,  $V_0$ , a, and b are the same as for the m = 4, n = 5 state of Table II.  $\lambda_{45}^{i,ex} = -9.371$ ,  $\lambda_{45}^{i,ex} = -8.790$ .

<sup>&</sup>lt;sup>c</sup> See Ref. c of Table II with  $\eta = 0.4$  replaced by  $\eta = 0.6$ .

d See Ref. d of Table II.

<sup>&</sup>lt;sup>b</sup> E,  $V_0$ , a, and b are the same as for the m = 4, n = 5 state of Table II.  $\lambda_{45}^{0,\text{ex}} = 33.36$ ,  $\lambda_{45}^{0,\text{ex}} = 33.67$ .

<sup>°</sup>See Ref. c of Table II with  $\eta = 0.4$  replaced by  $\xi = 1.0$ .

d See Ref. d of Table II.

<sup>&</sup>lt;sup>b</sup> E,  $V_0$ , a, and b are the same as for the m = 4, n = 5 state of Table II.

**TABLE VI.** Relative values of  $R_{mn}^{i}(\xi)$ 's for various  $\xi$ 's.

	m=5,n	$=6^{a}$	$m = 4, n = 5^{\rm b}$		
É	Semiclassical	Exact	Semiclassical <sup>c</sup>	Exact	
0.05	3.24( - 2) <sup>d</sup>	3.18( - 2)	3.38(-2)	3.35(-2)	
0.10	6.25(-2)	6.14(-2)	6.51(-2)	6.48(-2)	
0.15	8.80(-2)	8.68(-2)	9.19(-2)	9.16(-2)	
0.20	1.07(-1)	1.06(-1)	1.12(-1)	1.12(-1)	
0.25	1.18(-1)	1.18(-1)	1.24(-1)	1.24(-1)	
0.30	1.20(-1)	1.20(-1)	1.27(-1)	1.27(-1)	
0.35	1.13(-1)	1.13(-1)	1.20(-1)	1.20(-1)	
0.40	9.59(-2)	9.73(-2)	1.04(-1)	1.04(-1)	
0.45	7.13(-2)	7.31(-2)	8.02(-2)	7.99(-2)	
0.50	4.08(-2)	4.29(-2)	5.00(-2)	4.93(-2)	

<sup>&</sup>lt;sup>a</sup> E,  $V_0$ , a, and b are the same as for the m = 5, n = 6 state of Table II.  $\lambda_{56}^{\text{lex}} = -0.111$ ,  $\lambda_{56}^{\text{lex}} = 0.562$ .

been made for the variety of orientations examined here. Such a study should include the role of the solvent molecules, e.g., via a superexchange mechanism, and such molecular orbital-based calculations do not appear to be available as yet.

#### VI. CONCLUSION

A semiclassical plus single-term approximation for calculating the electron transfer matrix element  $H_{BA}$  has been formulated. It was shown to yield good agreement with results<sup>4</sup> in which the exact solution of the Schrödinger equation for the same model potential was used. This method also has much greater computational efficiency. In future applications of the model of Ref. 3 to the calculation of mutual orientation and separation distance effects, use of this method should be appropriate.

#### **ACKNOWLEDGMENTS**

It is a pleasure to acknowledge support of this research by the Office of Naval Research. RJC gratefully acknowledges the support of a National Science Foundation Predoctoral fellowship, 1979–1982. SJK gratefully acknowledges the support of a Natural Sciences and Engineering Research Council of Canada postgraduate scholarship, 1984–1985. The calculations reported in this paper made use of the Dreyfus-NSF theoretical chemistry computer which was funded through grants from the Camille and Henry Dreyfus Foundation, the National Science Foundation, and the Sloan Fund of the California Institute of Technology.

# APPENDIX A: PRESCRIPTION FOR CALCULATING THE $R_{mn}$ 's, $S_{mn}$ 's, $\lambda_{mn}$ 's AND $H_{BA}$

To facilitate use of the present method, details are given here on the calculation of  $H_{BA}$ . To this end, the  $R_{mn}$ 's,  $S_{mn}$ 's and  $\lambda_{mn}$ 's are calculated first, for any given E and V.

In obtaining a uniform semiclassical solution for  $S_{mn}^o$ ,  $S_{mn}^o$  is converted 12,17 to a function  $(1-\eta^2)^{1/2}S_{mn}^o$ , whose

differential equation contains no first derivatives. The comparison function chosen for making the uniform approximation is  $(1-v^2)^{1/2}P_l^m(v)$ , where  $P_l^m(v)$  is the associated Legendre function. Thereby, we have

$$S_{mn}^{o}(\eta) \simeq A \frac{(1-v^2)^{1/2}}{(1-\eta^2)^{1/2}} P_l^m(v),$$
 (A1)

where A is a constant which normalizes  $S_{mn}^{o}(\eta)$ , and where the function  $\nu(\eta)$  is defined below.

The mapping  $\eta \rightarrow \nu(\eta)$  leads in a standard way<sup>12,18</sup> to the equation

$$\int_{-\eta_{TP}}^{+\eta_{TP}} p_{\eta} \ d\eta = \int_{-\nu_{TP}}^{\nu_{TP}} p_{\nu} \ d\nu, \tag{A2}$$

where  $p_{\eta}$  is the classical  $\eta$  momentum

$$p_{\eta}^{2} = \frac{\lambda_{mn}^{o} + \eta^{2} d^{2} k_{0}^{2} / 4}{(1 - \eta^{2})} - \frac{(m^{2} - 1)}{(1 - \eta^{2})^{2}},$$
 (A3)

and  $p_{\nu}$  is the classical  $\nu$  momentum

$$p_{\nu}^{2} = \frac{l(l+1)}{1-\nu^{2}} - \frac{(m^{2}-1)}{(1-\nu^{2})^{2}},$$
 (A4)

with l=n. At  $\eta=\pm\eta_{TP}$ ,  $p_{\eta}=0$  while  $p_{\nu}=0$  at  $\nu=\pm\nu_{TP}$ . The left-hand side of Eq. (A2) was evaluated numerically, using a standard routine. The right-hand side equals  $\{[l(l+1)]^{1/2}-(m^2-1)^{1/2}\}\pi$ . The quantized value of  $\lambda_{mn}^o$  which appears in Eq. (A3) is that which permits Eq. (A2) to be satisfied.

The  $\nu$  in Eq. (A1) is given by Eq. (A2) with the upper (or lower) limits of integration on each side of the equation replaced by  $\eta$  and  $\nu(\eta)$ .<sup>19</sup> (The choice of which set of turning points to use is a matter of convenience in performing the integration. In principle either choice will suffice.) With this  $\nu(\eta)$  the  $S_{mn}^o(\eta)$  given in Eq. (A1) was calculated for subsequent use in the calculation of  $H_{BA}$ .

The function  $R_{mn}^{o}(\xi)$ , the "radial" function outside the potential well, satisfies Eq. (4c), with the *i* superscripts and subscripts there replaced by o's. In the present study the following primitive semiclassical approximation<sup>12,17</sup> for  $R_{mn}^{o}(\xi)$  sufficed because of the absence of turning points for the  $\xi$  motion:

$$R_{mn}^{o}(\xi) \simeq \left[ \exp \left( - \int_{\xi_0}^{\xi} |p_{\xi}| d\xi \right) \right] / (\xi^2 + 1)^{1/2} |p_{\xi}|^{1/2},$$
(A5)

where the classical  $\xi$  momentum  $p_{\xi}$  is defined by

$$p_{\xi}^{2} = c_{o}^{2} - \{ [(c_{o}^{2} + \lambda_{mn}^{o})(\xi^{2} + 1) - (m^{2} - 1)]/(\xi^{2} + 1)^{2} \},$$

with  $c_o^2 = d^2 k_o^2/4$  and where  $\lambda_{mn}^o$  was calculated above.

The calculation of  $\lambda_{mn}^{i}$  and  $S_{mn}^{i}$  is lengthier and is discussed at the end of this Appendix.

The inner radial function  $R_{mn}(\xi)$  satisfies Eq. (4c). The tendency towards an absence of turning points, i.e., for the effective energy for the  $\xi$  motion to exceed the effective potential energy for all  $\xi$ , increases with increasing d, increasing  $k_i^2$  and decreasing n. For the  $(m,\pi)$  states and choice of parameters appropriate to the modeling of large aromatic systems discussed here there are no turning points for the  $\xi$  motion in the region  $\xi \leqslant \xi_0$ , and so a primitive semi-

<sup>&</sup>lt;sup>b</sup> E,  $V_0$ , a, and b are the same as for the m=4, n=5 state of Table II.  $\lambda_{45}^{lex} = -9.37$ ,  $\lambda_{45}^{lex} = -8.73$ .

<sup>°</sup> See Ref. c of Table II with  $\eta = 0.4$  replaced by  $\xi = 0.30$ .

d See Ref. d of Table II.

classical approximation suffices for  $R_{mn}^{i}(\xi)$ . The boundary condition for  $\pi$ -like states is that the wave function be zero in the xy plane. Thereby, it is also zero on the disk of diameter d, centered at the origin, in the xy plane, and hence at  $\xi = 0$ . (It is also zero at  $\eta = 0$ .) The primitive semiclassical  $R_{mn}^{i}(\xi)$  satisfying this condition is

$$R_{mn}^{i}(\xi) \simeq \left[ \sin \left( \int_{0}^{\xi} |p_{\xi}| d\xi \right) \right] / (\xi^{2} + 1)^{1/2} |p_{\xi}|^{1/2},$$
(A6)

where  $p_{\xi}^2$  is the same as that given following Eq. (A5), but with o subscripts and superscripts replaced by i's.

All the components of  $\Psi^o_{m,m+1}$  and  $\Psi^i_{m,m+1}$  have now been considered  $[\Phi^{i,o}_m(\varphi) = B \cos m\varphi + C \sin m\varphi]$ , with appropriate normalization] and thus the next step is to satisfy the quantization conditions. This is done by choosing the desired value of E and then using a root search technique (we used the Newton-Raphson method) to find the value of the well depth  $V_0$  which allows Eq. (7) of the text to be satisfied.  $C^o_{m+1}$ , and  $C^i_{m+1}$  are determined using Eq. (6a) and normalizing the  $\Psi_{m,\pi}$  defined in Eq. (5) of the text. The entire procedure is followed for both wells A and B.  $H_{BA}$  can then be calculated straightforwardly from Eq. (3b) of the text using nested numerical integration to perform the three-dimensional integral. We note that the integration only needs to be performed over well B, since this is the only region where  $V^B$  is nonzero.

In the above discussion we deferred consideration of  $S_{mn}^{i}$  and  $\lambda_{mn}^{i}$ . We now treat them by first describing a new procedure for defining localized wave functions.

First introducing<sup>12</sup> the function  $U^{i}_{mn}(\eta) = (1 - \eta^2)^{1/2} S^{i}_{mn}(\eta)$ , as noted earlier, then using<sup>20</sup> the Bethe modification, namely, substituting  $m^2$  for  $m^2 - 1$ , we obtain an equation for  $U^{i}_{mn}(\eta)$ :

$$\frac{d^{2}}{d\eta^{2}}U_{mn}^{i}(\eta) - V^{\text{eff}}(\eta)U_{mn}^{i}(\eta) = 0, \tag{A7}$$

where

$$V^{\text{eff}}(\eta) = \left[ m^2 - (\lambda_{mn}^i + c_i^2 \eta^2) (1 - \eta^2) \right] / (1 - \eta^2)^2,$$

with

$$c_i^2 \equiv d^2 k_i^2 / 4 = d^2 \mu (E + V_0) / 2\hbar^2$$
.

This  $V^{\rm eff}(\eta)$  serves as an effective "V-E" term for the  $\eta$  motion.

When  $c_i^2$  is zero the numerator in  $V^{\text{eff}}(\eta)$  is quadratic in  $\eta$ . For  $c_i^2 \neq 0$ , this numerator is a quartic function which, for large enough  $c_i^2$ , has four real zeros. Examples of plots of  $V^{\text{eff}}(\eta)$  for various positive values of  $V_0$  and thus for various  $c_i^2$ 's are given in Fig. 7. It is seen that as  $V_0$  and thus as  $c_i^2$  increases,  $V^{\text{eff}}(\eta)$  changes from having two zeros to having four. For the states of interest in the present paper  $V^{\text{eff}}(\eta)$  in Eq. (A7) typically has four zeros (i.e., the problem has four turning points), and we devised the following method for obtaining  $S_{mn}^i$ . [Had there been only two turning points an equation analogous to Eq. (A1) for  $S_{mn}^o(\eta)$  would have been appropriate.]

In principle, a four turning-point problem can be treated with a comparison function that arises from a potential which itself yields four turning points, but such functions are typically as complicated as  $S^i_{mn}(\eta)$  itself. Accordingly, results for two single-well problems were used, noting that the eigenvalues of a symmetric double well potential for a high barrier occur in pairs and the eigenfunctions can be represented to a high degree of accuracy by symmetric and antisymmetric combinations of the single-well wave functions. Single-well potentials were devised for the portions of the wave function localized to the left- and the right-hand side of  $\eta = 0$ . Linear combinations of two semiclassical single-well eigenfunctions then yielded an approximate  $S^i_{mn}(\eta)$ .

For this purpose we introduce an effective single-well  $V_l^s(\eta)$  to replace  $V^{\text{eff}}(\eta)$ , so as to yield a wave function largely localized in the  $(-1 \le \eta \le 0)$  region, (cf. Fig. 8)<sup>22</sup>:

$$V_{i}^{s}(\eta) = \begin{cases} \frac{m^{2} - (\lambda_{mn}^{i} + c_{i}^{2}\eta^{2})(1 - \eta^{2})}{(1 - \eta^{2})^{2}} & (-1 \leqslant \eta \leqslant 0), (\eta_{i} \leqslant \eta \leqslant 1) \\ (1 - \eta^{2})^{2} & , \end{cases}$$

$$V_{i}^{s} \qquad (0 \leqslant \eta \leqslant \eta_{i})$$
(A8)

where  $V^s$  equals  $m^2 - \lambda_{mn}^i$  and  $\eta_i$  is the  $\eta$  in the interval (0,1) where  $V_l^s(\eta_i) = V^s$ . The single-well potential for a wave function localized between  $0 < \eta \le 1$  is simply the reflection of the potential depicted in Fig. 8 about  $\eta = 0$ . Each of these effective single-well potentials yields a two-turning point problem which can be solved using a uniform approximation based on a comparison equation for the two-turning point problem. The harmonic oscillator equation was chosen for the latter. A zeroth order separation constant  $\lambda_{mn}^i$  is then obtained semiclassically from the single-well problem in a way analagous to the determination of  $\lambda_{mn}^o$ . The analog of Eq. (A2) for the determination of  $\lambda_{mn}^i$  is

$$\int_{-\eta_{TP}^{1}}^{\eta_{TP}^{2}} \left[ V_{l}^{s}(\eta) \right]^{1/2} d\eta = \int_{-x_{TP}}^{+x_{TP}} \left[ (2N+1) - \frac{x^{2}}{2} \right]^{1/2} dx$$

$$= (2N+1) \frac{\pi}{2}, \qquad (A9)$$

where  $V_l^s(\eta)$  is defined in Eq. (A8),  $x_{TP}$  is the x for which the x integrand vanishes, and the  $\eta_{TP}^{1,2}$ 's are the values of  $\eta$  for which the  $\eta$  integrand vanishes. The first integral in Eq. (A9) was evaluated numerically, choosing  $\lambda_{mn}^l$  so as to satisfy Eq. (A9).

The choice of the quantum number N for the harmonic oscillator comparison wave function  $\varphi_N(x)$  is determined by the state to be modeled. The number of nodes for the function  $S^i_{mn}(\eta)$  (excluding those at  $\eta=\pm 1$ ) is n-m. Thereby,  $S^i_{m,m}(\eta)$  has no nodes, while  $S^i_{m,m+1}(\eta)$  has one. The number of nodes of  $\varphi_N(x)$  is N. Since pairs of  $\varphi_N$ 's are combined, one member from each well,  $S^i_{m,m}$  states are obtained by taking the symmetric combination of two groundstate harmonic oscillator-like wave functions,  $\varphi_0(x)$ , regardless of the value of m. For a  $\pi$  state, we need consider only states where n=m+1.  $S^i_{m,m+1}$  is obtained by taking

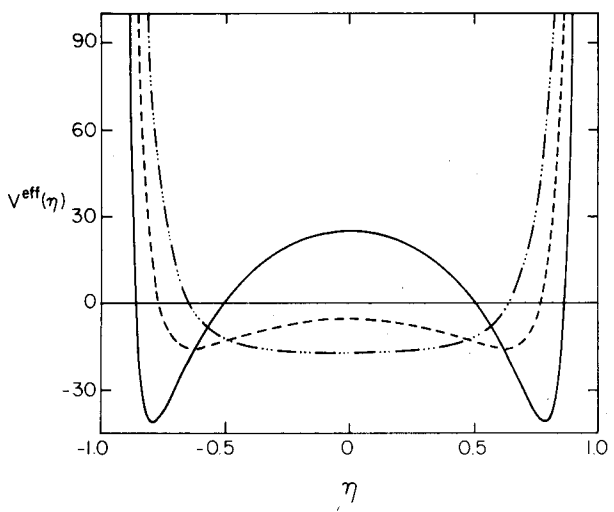


FIG. 7. Effective potential for  $S^i_{mn}$  as a function of  $\eta$  for three different values of  $V_0$ . The other parameters used in all 3 plots are a=5 Å, b=2 Å, m=5, n=6, and E=-2.8 eV. — corresponds to  $V_0=26.3022$  eV and  $\lambda^i_{56}=0.3807$ . --- corresponds to  $V_0=12.00$  eV and  $\lambda^i_{56}=30.60$ . ---- corresponds to  $V_0=3.00$  eV and  $\lambda^i_{56}=42.02$ .

the antisymmetric combination of the two  $\varphi_0(x)$  wave functions. (Similar reasoning shows that for  $S_{mn}^i$  states for which n > m + 1, and when there are four turning points, linear combinations of two  $\varphi_N$ 's with N = 1, 2, ..., would be used.)

Thus  $S_{m,m+1}^{i}$  is then given by

$$S_{m,m+1}^{i}(\eta) = \frac{A}{(1-\eta^2)^{1/2}} [U_l(\eta) - U_r(\eta)], \text{ (A10)}$$

where  $U_l(\eta)$  is  $\exp(-x_l^2(\eta))$ , i.e., a ground state harmonic oscillator wave function in the new variable  $x_l(\eta)$  for the left-hand side single well;  $x_l(\eta)$  is defined by Eq. (A9) with the upper or lower integration limits replaced by  $\eta$  and  $x_l(\eta)$ .<sup>24</sup> Similar definitions apply to  $U_r(\eta)$  and  $x_r$ , but with l's replaced by r's and with  $V_r^s(\eta)$  as the single-well potential for a wave function "localized" in  $0 \le \eta \le 1$ . A is a constant which normalizes  $S_{m,m+1}^i(\eta)$ .

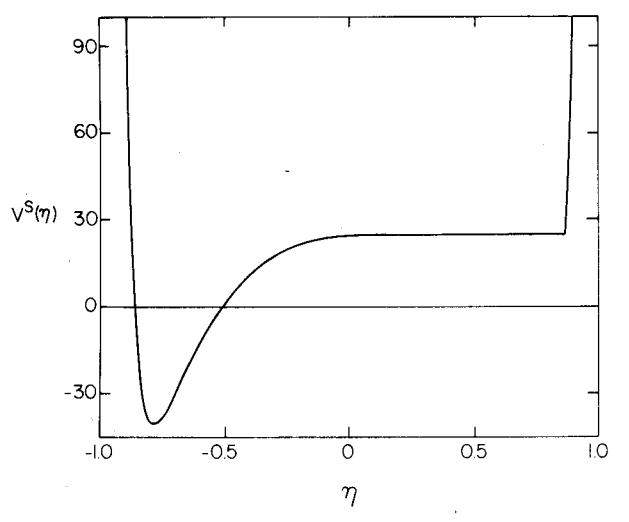


FIG. 8. Effective single-well potential for a localized  $S_{mn}^{i}$  state, localized between  $-1 < \eta < 0$  as a function of  $\eta$ . The parameters a, b, m, n, and E are the same as in Fig. 7, and  $V_0 = 26.3022$  eV.

The above  $\lambda_{m,m+1}^i$ 's can be termed zeroth order  $\lambda_{m,m+1}^i$ 's. We also calculated "corrected"  $\lambda_{m,m+1}^i$ 's which allow for the splitting of the eigenvalues by tunneling in the double-well problem. To do this we use the above  $U_I$  and  $U_r$  as basis functions, and obtain solutions of Eq. (A7) by solving

$$\begin{bmatrix} F_{ll} F_{lr} \\ F_{rl} F_{rr} \end{bmatrix} \begin{bmatrix} c_1 \\ c_2 \end{bmatrix} = \lambda \begin{bmatrix} 1 & G_{lr} \\ G_{rl} & 1 \end{bmatrix} \begin{bmatrix} c_1 \\ c_2 \end{bmatrix},$$
(A11)

where  $F_{ij}$  denotes the matrix element  $\langle U_i | F | U_j \rangle$  of

$$F = (1 - \eta^2)(d^2/d\eta^2) + [m^2/(1 - \eta^2)] - c_i^2 \eta^2$$

and  $G_{ij}$  denotes  $\langle U_i | U_j \rangle$ . Equation (A11) yields two eigenvalues  $\lambda_{m,m}$  and  $\lambda_{m,m+1}$ . This corrected  $\lambda_{m,m+1}^i$  was used in the calculation of  $R_{m,m+1}^i$  utilizing Eq. (A6)<sup>25</sup> and so to obtain the results given in the various tables and figures. However, we have found that for the parameters and states employed here, use of the zeroth order  $\lambda_{m,m+1}^i$ , i.e., values without the splitting, gave results for the  $R_{mn}^i$ 's which differed negligibly in the domain of interest and hence could have been used instead.

## APPENDIX B: SEMICLASSICAL ENERGY EIGENVALUES

Using the semiclassical approximations to the individual  $R_{mn}$ 's and  $S_{mn}$ 's, and inside and outside the well, together with the single-term approximation, the energy values can be calculated using Eqs. (6) and (7) for given values of the potential and for various states. When  $V_0$ , a, and b for m=5, n=6 were chosen to be the values in Table II (Ref. a), the exact value of E was -2.8 eV, but the approximate value was -3.46 eV. To obtain the desired E of -2.8 eV in the approximate quantization, a  $V_0$  of 25.5316 eV was needed and was used. When  $V_0$ , a, and b for m=4, n=5 were chosen to be the values in Table II (Ref. b) the exact value of E was -2.8 eV, while the approximate value was -3.39 eV. To obtain the desired E of -2.8 eV in the approximate quantization, a  $V_0$  of 21.4993 eV was needed and used.

There is seen to be a fairly large error in this calculated eigenvalue, a result not unexpected, because of the observed contribution of several terms to the total wave functions near the well boundary. As was seen previously, however, these single-term functions are still accurate enough to yield reasonable results for  $H_{BA}$ .

Brocklehurst, J. Phys. Chem. 83, 536 (1979); (c) A. B. Doktorov, R. F. Khairutdinov, and K. I. Zamaraev, Chem. Phys. 61, 351 (1981).

<sup>&</sup>lt;sup>1</sup>R. A. Marcus and N. Sutin, Biochim. Biophys. Acta. **811**, 265 (1985). <sup>2</sup>(a) S. A. Rice and M. J. Pilling, Prog. React. Kinet. **9**, 93 (1978); (b) B.

<sup>&</sup>lt;sup>3</sup>P. Siders, R. J. Cave, and R. A. Marcus, J. Chem. Phys. **81**, 5613 (1984). <sup>4</sup>R. J. Cave, P. Siders, and R. A. Marcus, J. Phys. Chem. (submitted).

<sup>&</sup>lt;sup>5</sup>C. Flammer, Spheroidal Wave Functions (Stanford University, Stanford, CA, 1957).

<sup>&</sup>lt;sup>6</sup>V. G. Levich and R. R. Dogonadze, Collect. Czech. Chem. Commun. 26, 193 (1961); English Translation, O. Boshko, University of Ottawa, Ontario, Canada.

<sup>&</sup>lt;sup>7</sup>R. R. Dogonadze, A. M. Kuznetsov, and M. A. Vorotyntsev, Phys. Status Solidi B **54**, 125 (1972), **54**, 425 (1972).

 <sup>&</sup>lt;sup>8</sup>N. R. Kestner, J. Logan, and J. Jortner, J. Phys. Chem. 78, 2148 (1974).
 <sup>9</sup>B. S. Brunschwig, J. Logan, M. D. Newton, and N. Sutin, J. Am. Chem. Soc. 102, 5798 (1980).

<sup>&</sup>lt;sup>10</sup>P. Siders and R. A. Marcus, J. Am. Chem. Soc. 103, 741 (1981).

<sup>&</sup>lt;sup>11</sup>D. B. Hodge, J. Math. Phys. 11, 2308 (1970).

<sup>12</sup>M. L. Sink and B. C. Eu, J. Chem. Phys. 78, 4887 (1983).

<sup>13</sup>Sink and Eu (Ref. 12) treated the analogous prolate spheroidal problem, related to the present  $S_{mn}^o$  and  $R_{mn}^o$ . There are a number of differences between our treatment and theirs: (a) They do not have a boundary  $\xi_0$  and hence do not need the "inner" wave functions. (b) They make the Langer modification [R. E. Langer, Phys. Rev. 51, 669 (1937), M. S. Child, Molecular Collision Theory (Academic, New York, 1974), p. 44], i.e., they set  $l(l+1) \rightarrow (l+1)^2$  whereas we do not. (c) They also make an adjusted Bethe modification (Ref. 12) [H. A. Bethe, Hand. Physik 24 Part 1, 273 (1933) (cf. Ref. 2, p. 411)]  $(m^2 - 1) \rightarrow (m + d)^2$ , where d is a small positive constant chosen to give the best approximate  $\lambda_{mn}^{o}$ 's. We comment on these differences as follows: (a) The presence of the boundary leads to our having to treat the four turning-point problem. (b) When the Langer modification is avoided the  $S_{mn}^{o}$  reduce asymptotically to the coresponding  $P_{I}^{m}$ , as  $n \to \infty$ . [The difference between using and not using the Langer modification is quite small (<0.1% in  $S_{mn}^o$ ) for the states examined here. 1 (c) The interest of Sink and Eu was in constructing a single uniform approximation for all mn states. Had they not adjusted the Bethe modification their method would not have yielded a single-valued mapping function for the case of n = m = 0. In the present case, where only high n and m states are considered, the question of single valuedness for the mapping variable did not arise and a Bethe modification for Some was not needed. The Bethe modification for the  $\eta$  spheroidal equation is used when a harmonic oscillator comparison function is used, for the latter involves a mapping of the interval (-1,1) onto the infinite interval  $(-\infty,\infty)$ . Accordingly, we used the Bethe modification for  $S_{mn}^i$  but not for  $S_{mn}^{o}$ , since we used an associated Legendre comparison function for  $S_{mn}^{o}$  rather than a harmonic oscillator comparison function.

14Of this factor of 50, a factor of 20 simply arises from the use of the single-term wave function and a factor of about 2.5 from the use of the semiclassical approximations in the wave functions.

<sup>15</sup>M.-H. Whangbo and K. R. Stewart, Isr. J. Chem. 23, 133 (1983).

<sup>16</sup>W. J. Pietro, D. E. Ellis, T. J. Marks, and M. A. Ratner, Mol. Cryst. Liq. Cryst. 105, 273 (1984).

<sup>17</sup>S. S. Gershtein, L. I. Ponomarev, and T. P. Puzyninca, Sov. Phys. JETP **21**, 418 (1965). These authors treated the analogous prolate spheroidal problem, and for it they justified the replacement of  $m^2 - 1$  in Eqs. (A3) and (A4) by  $m^2$  (Bethe modification).

<sup>18</sup>Uniform semiclassical treatments for second order differential equations having no first derivatives are discussed by S. C. Miller, Jr. and R. H. Good, Jr., Phys. Rev. **91**, 174 (1953); A. Erdélyi, J. Math. Phys. **1**, 16 (1960)

<sup>19</sup>The values of the  $\nu$  integrals are then as follows. For  $|\nu| > |\nu_{TP}|$ :

$$\int_{\pm |\nu_{TP}|}^{\pm |\nu|} p_{\nu} d\nu = \frac{i(m^2 - 1)^{1/2}}{2} \times \ln \left\{ \frac{(m^2 - 1)^{1/2} \nu + [(m^2 - 1) - l(l + 1)(1 - \nu^2)]^{1/2}}{(m^2 - 1)^{1/2} \nu - [(m^2 - 1) - l(l + 1)(1 - \nu^2)]^{1/2}} \right\}$$

$$-i[l(l+1)]^{1/2} \times \ln \left| \frac{[(m^2-1)-l(l+1)(1-\nu^2)]^{1/2} + [l(l+1)]^{1/2} \nu}{[l(l+1)-(m^2-1)]^{1/2}} \right|.$$

For  $-\nu_{TP} < \nu < \nu_{TP}$ :

$$\int_{-v_{TP}}^{v} p_{v} dv = \left\{ [l(l+1)]^{1/2} - (m^{2} - 1)^{1/2} \right\} \frac{\pi}{2}$$

$$- (m^{2} - 1)^{1/2}$$

$$\times \arctan \left\{ \frac{v(m^{2} - 1)^{1/2}}{[l(l+1)(1 - v^{2}) - (m^{2} - 1)]^{1/2}} \right\}$$

$$+ [l(l+1)]^{1/2}$$

$$\times \arcsin \left\{ \frac{v[l(l+1)]^{1/2}}{[l(l+1) - (m^{2} - 1)]^{1/2}} \right\}.$$

<sup>20</sup>H. A. Bethe, Ref. 13.

<sup>21</sup>M. A. Morrison, T. L. Estle, and N. F. Lane, Quantum States of Atoms, Molecules, and Solids (Prentice-Hall, New Jersey, 1976), p. 276.

<sup>22</sup>This procedure has elements in common with that used by V. Lopez, V. K. Babamov, and R. A. Marcus [J. Chem. Phys. 81, 3962 (1984)] for a different double-well problem.

<sup>23</sup>Unlike the case of  $S_{mn}^o$ , the associated Legendre equation was not used. The single-well solutions are quite different from associated Legendre functions.

<sup>24</sup>The x integrals are then as follows: For  $|x| > |x_{TP}|$ :

$$\int_{\pm |x_{TP}|}^{\pm |x|} p_x \, dx = \frac{ix}{2} \left[ x^2 - (2N+1) \right]^{1/2} - i(N+1/2) \ln \left| \frac{x + \left[ x^2 - (2N+1) \right]^{1/2}}{\left[ (2N+1) \right]^{1/2}} \right|.$$

For  $-x_{TP} < x < x_{TP}$ :

$$\int_{-x_{TP}}^{x} p_x dx = \frac{x}{2} \left[ (2N+1) - x^2 \right]^{1/2} + (N+1/2) \times \arcsin \left[ \frac{x}{(2N+1)^{1/2}} \right] + (N+1/2) \frac{\pi}{2}.$$

<sup>25</sup>The zeroth order  $\lambda_{mn}^{i}$ 's are used for the  $S_{mn}^{i}$ 's, in order that the zeros of the comparison function and the original function  $U_{mn}^{i}$ , are mapped onto one another by Eq. (A9).